



High Abundance of Intratumoral $\gamma\delta$ T Cells Favors a Better Prognosis in Head and Neck Squamous Cell Carcinoma: A Bioinformatic Analysis

Huanzi Lu[†], Wenxiao Dai[†], Junyi Guo, Dikan Wang, Shuqiong Wen, Lisa Yang, Dongjia Lin, Wenqiang Xie, Liling Wen, Juan Fang and Zhi Wang*

Hospital of Stomatology, Guanghua School of Stomatology, Guangdong Provincial Key Laboratory of Stomatology, Sun Yat-sen University, Guangzhou, China

OPEN ACCESS

Edited by:

Jianlei Hao,
Jinan University, China

Reviewed by:

Zheng Xiang,
The University of Hong Kong,
Hong Kong
Oscar Junhong Luo,
Jinan University, China

*Correspondence:

Zhi Wang
wangzh75@mail.sysu.edu.cn

[†]These authors have contributed
equally to this work

Specialty section:

This article was submitted to
T Cell Biology,
a section of the journal
Frontiers in Immunology

Received: 18 June 2020

Accepted: 01 September 2020

Published: 30 September 2020

Citation:

Lu H, Dai W, Guo J, Wang D, Wen S,
Yang L, Lin D, Xie W, Wen L, Fang J
and Wang Z (2020) High Abundance
of Intratumoral $\gamma\delta$ T Cells Favors a
Better Prognosis in Head and Neck
Squamous Cell Carcinoma: A
Bioinformatic Analysis.
Front. Immunol. 11:573920.
doi: 10.3389/fimmu.2020.573920

$\gamma\delta$ T cells are a small subset of unconventional T cells that are enriched in the mucosal areas, and are responsible for pathogen clearance and maintaining integrity. However, the role of $\gamma\delta$ T cells in head and neck squamous cell carcinoma (HNSCC) is largely unknown. Here, by using RNA-seq data from The Cancer Genome Atlas (TCGA), we discovered that HNSCC patients with higher levels of $\gamma\delta$ T cells were positively associated with lower clinical stages and better overall survival, and high abundance of $\gamma\delta$ T cells was positively correlated with CD8⁺/CD4⁺ T cell infiltration. Gene ontology and pathway analyses showed that genes associated with T cell activation, proliferation, effector functions, cytotoxicity, and chemokine production were enriched in the group with a higher $\gamma\delta$ T cell abundance. Furthermore, we found that the abundance of $\gamma\delta$ T cells was positively associated with the expression of the butyrophilin (BTN) family proteins BTN3A1/BTN3A2/BTN3A3 and BTN2A1, but only MICB, one of the ligands of NKG2D, was involved in the activation of $\gamma\delta$ T cells, indicating that the BTN family proteins might be involved in the activation and proliferation of $\gamma\delta$ T cells in the tumor microenvironment of HNSCC. Our results indicated that $\gamma\delta$ T cells, along with their ligands, are promising targets in HNSCC with great prognostic values and treatment potentials.

Keywords: head and neck squamous cell carcinoma (HNSCC), $\gamma\delta$ T cells, butyrophilin, BTN3A1, MICB, TCGA, ImmuCellAI, CIBERSORTx

INTRODUCTION

Head and neck cancer is a group of cancers that occurs in the head and neck region, including the oral cavity, pharynx and larynx, of which more than 90% cases are squamous cell carcinoma (1). Head and neck squamous cell carcinoma (HNSCC) is the seventh most common cancer globally in 2018, accounting for 3% of all cases of cancer incidence and 1.5% of all cancer deaths annually (2). Although the treatment of HNSCC has evolved from surgery to a multidisciplinary treatment including surgery, radiotherapy, chemotherapy and molecular targeted therapy in the past few decades, the 5-year overall survival (OS) of HNSCC patients has not been significantly improved, remaining at ~60% (3). In addition, more than 50% of HNSCC patients have a locoregional recurrence or distant metastasis within 3 years, which results in a poorer prognosis (4). In recent years, with the advancement of cancer immunotherapy, some patients with advanced cancer have

benefited from it, but the response rate in HNSCC patients is only ~13–20% (4, 5). Therefore, it is urgent to find novel molecular markers or cell types with therapeutic and prognostic values in HNSCC.

T cells are a group of immune cells that play the key role in antitumor immune response. Based on the composition of T cell receptors (TCR), T cells are mainly divided into $\alpha\beta$ T cells and $\gamma\delta$ T cells (6). $\alpha\beta$ T cells, including CD4+ T cells and CD8+ T cells, have been extensively studied in tumor immunity, but the role of $\gamma\delta$ T cells in the tumor microenvironment (TME) is largely unknown. $\gamma\delta$ T cells account for only 1–5% of total T cells in the peripheral blood, but they mainly reside in mucosal areas, such as the intestinal epithelia and oral mucosa, accounting for 10–100% of intraepithelial lymphocytes (7). Generally, $\gamma\delta$ T cells are responsible for pathogen clearance and maintaining integrity of the epithelium (7). According to the arrangement of the V δ chain, human $\gamma\delta$ T cells are classified into three different subsets, namely V δ 1 T cells, V δ 2 T cells, and V δ 3 T cells which are only found in liver (8). V δ 2 T cells are the main subset of circulating $\gamma\delta$ T cells in the peripheral blood, accounting for about 50 ~ 90% $\gamma\delta$ T cells (9). In addition, V δ 2 T cells also accumulate in tumor tissues and exert potent cytotoxic activity, indicating that these cells possess a potential antitumor activity. In contrast, V δ 1 T cells are mainly distributed in mucosal areas, playing an important role in killing bacteria or viruses and maintaining tissue homeostasis, in addition, they are also involved in antitumor immunity (10).

Recent studies have reported that the infiltration level of cytotoxic T cells or NK cells in the TME is usually correlated with an improved prognosis in various kinds of cancers (11). $\gamma\delta$ T cells, as one of the cytotoxic T cells that infiltrates tumor tissue, are reported to possess a high cytotoxic activity in lung cancer, breast cancer, colon cancer and gastric cancer, and are related to the improvement of overall survival (12). However, recent studies showed that $\gamma\delta$ T cells may also promote tumor progression (13). However, until now, the functions and prognostic value of $\gamma\delta$ T cells in HNSCC have been rarely studied. A previous study explored the $\gamma\delta$ T cells in the peripheral blood of HNSCC patients and found that there was no correlation between $\gamma\delta$ T cell abundance and T stages (14), but the abundance of $\gamma\delta$ T cells in the TME has not been studied.

Unlike conventional T cells, which recognize antigens presented by tumor cells or antigen presenting cells (APC) through major histocompatibility complex (MHC) molecules, $\gamma\delta$ T cells recognize various types of antigens without MHC restriction (15), but the exact mechanisms that trigger $\gamma\delta$ T cell activation and proliferation are largely unknown. Notably, recent studies have found that V δ 2 T cells are activated by phosphoantigens (P-Ags) produced by malignant cells or infected cells through the presentation of butyrophilin family proteins (BTNs) to TCR $\gamma\delta$ on V δ 2 T cells (16). BTNs belong to the type I transmembrane proteins of the immunoglobulin superfamily. In humans, these proteins can be classified into BTN1, BTN2, and BTN3 subfamilies, including BTN1A1, BTN2A1-2, and BTN3A1-3 (17). Among them, BTN2A1 and BTN3A1-3 have been reported to take up and present P-Ags to the TCR of $\gamma\delta$ T cells (18–20). Studies have shown that through the binding to P-Ags presented by BTN3A1 and BTN2A1 on infected or malignant

cells, $\gamma\delta$ T cells could be activated, proliferate rapidly, and release cytokines to induce anti-infection or antitumor responses (20, 21). Recent studies have found that a higher expression of BTN3A2 in ovarian cancer and triple negative breast cancer is positively correlated with increased T cell infiltration and a better prognosis (22, 23), but other studies have reported that BTN3A2 is associated with poor prognosis in gastric cancer and pancreatic ductal adenocarcinoma (PDAC) (22, 24). In addition, the engagement of natural killer group 2 member D (NKG2D) with its ligands provides the costimulatory signaling pathway that activates $\gamma\delta$ T cells (25). The NKG2D ligands (NKG2DLs) include MHC class I polypeptide-related sequence A and B (MICA/MICB) and the UL16 binding protein 1-6 (ULBP1-6) (26). However, the potential correlation of $\gamma\delta$ T cells and BTN families in the TME of HNSCC is still unclear, and whether the NKG2DL-NKG2D pathway participates in the antitumor immunity of HNSCC remains to be discovered.

In this study, by using the patient cohorts from TCGA database, we discovered that HNSCC patients with a higher abundance of $\gamma\delta$ T cells had prolonged overall survival, suggesting that $\gamma\delta$ T cells were of great prognostic values for HNSCC, and were highly correlated with CD8+ T cell and CD4+ T cell infiltration in the TME. We further found that activation of $\gamma\delta$ T cells in the TME was associated with the BTN family proteins. This study revealed the prognostic value of $\gamma\delta$ T cells in head and neck cancer, and revealed the possible activation mechanisms of $\gamma\delta$ T cells in HNSCC.

MATERIALS AND METHODS

HNSCC and CESC Datasets From TCGA Database

Data on the HNSCC patient cohort was downloaded from The Cancer Genome Atlas (TCGA). Patients without RNA-seq data were excluded. A total of 537 samples were included in this study, including 494 tumor tissue samples and 43 adjacent normal tissue samples, all of the 43 adjacent normal tissue samples were classified into normal group. The phenotype information and survival data of HNSCC patients (version: 08-07-2019) and RNA-seq data (version: 07-19-2019) were downloaded from UCSC Xena (<https://xenabrowser.net/datapages/>). In addition, the RNA-seq data (version: 07-19-2019), phenotype (version: 08-07-2019) data and survival data (version: 07-19-2019) of a cervical squamous cell carcinoma (CESC) patient cohort were also downloaded from UCSC Xena. Patients without RNA-seq data were excluded. A total of 281 samples were included in this study, including 278 tumor tissue samples and 3 adjacent normal tissue samples. The classification of T stage, N stage and clinical stage of each patient was based on American Joint Committee of Cancer (AJCC, 7th edition) (27). The RNA-seq data included Fragments per Kilobase Million (FPKM) matrix and a counts matrix and to reduce biases among different samples, the FPKM format was converted into a Transcripts Per Million (TPM) format for further analysis (28). The function for the conversion of FPKM to TPM is listed below, and this process was calculated by R language:

$TPM(i) = (FPKM(i)/\text{sum}(FPKM \text{ all transcripts})) \times 10^6$ (where i refers to the specific gene of specific sample in the expression matrix).

After conversion, the sum of all transcripts in each sample was on the order of 10^6 , which makes it more convincing to compare the expression levels of specific genes across different samples.

Gene Expression Comparison and Correlation Analysis

$\gamma\delta$ T cell abundance is defined by the geometric mean of the TPM values of TRDC/TRGC1/TRGC2, where TRDC encodes the constant chain of TCR δ , and TRGC1 and TRGC2 encode the constant chain of TCR γ . Based on the median expression of the geometric mean, the HNSCC patients were dichotomized into $\gamma\delta$ T-hi and $\gamma\delta$ T-lo groups (247 patients in each group, **Table 1**). Furthermore, to explore the effects of the BTN family proteins on the prognosis of HNSCC patients, the cohort was dichotomized based on the median expression levels of BTN3A1/BTN3A2/BTN3A3/BTN2A1, respectively. The effector and cytotoxic functions of $\gamma\delta$ T cells were assessed by the expression levels of IFNG (interferon- γ), GZMA (granzyme A), GZMB (granzyme B), and GNLY (granulysin). The activation degree of cytotoxic $\gamma\delta$ T cells is reflected by transcription factor Hobit (encoded by ZNF683) and activation receptor NKG2D (encoded by KLRK1). The difference in the ability to recruit CD8+ T cells between the $\gamma\delta$ T-hi and $\gamma\delta$ T-lo groups was shown by the expression levels of the chemokines CCL5 and CXCL9, which was reported previously (29). The expression levels of $\gamma\delta$ T cell activation ligands among the $\gamma\delta$ T-hi, $\gamma\delta$ T-lo and normal groups are shown by the expression levels of ligands that can be recognized and bound by TCR $\gamma\delta$ (BTN2A1, BTN3A1-3), and ligands that bind to NKG2D and activate $\gamma\delta$ T cells (MICA, MICB, and ULBP1-6). Boxplots, heatmap and scatter plots were drawn by using R packages ggplot2, ggpubr and pheatmap. In the boxplots, the center line of box represents the median value, the upper and lower edges of box indicate the 75th and 25th percentiles, respectively. The whiskers extend 1.5 times the interquartile range (IQR) beyond the 75th and 25th percentiles of the box, respectively. Student's t -test was used to compare the difference in gene expression values between the two groups. Linear regression analysis was used to compare the correlation between each ligand and the geometric mean of the $\gamma\delta$ T cell markers. For the linear regression analysis, the gene expression levels were first converted to $\log_{10}(TPM+1)$, and Pearson correlation coefficient R -values and P -values were obtained. Among these, the absolute value of R ($|R|$) > 0.7 was considered as a strong correlation, $0.4 < |R| < 0.7$ was considered as a moderate correlation, and $|R| < 0.4$ was considered as a weak correlation. $P < 0.05$ is considered to be statistically significant.

Estimation of the Relative Abundance of Immune Cells in the RNA-seq Data

The relative abundance of immune cells in the RNA-seq data of HNSCC and CESC patients was estimated by using the newly developed online tool ImmuCellAI (Immune Cell Abundance Identifier), which is comprised of 24 immune cells, including

TABLE 1 | Baseline and clinical information of HNSCC patients in TCGA database.

Factor		$\gamma\delta$ T-hi number(%)	$\gamma\delta$ T-lo number(%)	P -value
$\gamma\delta$ T cell marker expression (TPM)		0.60–19.03	0.00–0.59	
Gender	Male	179 (36.2%)	183 (37.0%)	0.684
	female	68 (13.8%)	64 (13.0%)	
Age	≥ 60 y	148 (30.0%)	130 (26.3%)	0.103
	< 60 y	99 (20.0%)	117 (23.7%)	
Smoking history	Yes	154 (31.2%)	149 (30.2%)	0.644
	No	93 (18.8%)	98 (19.8%)	
Alcohol history	Yes	167 (33.8%)	160 (32.4%)	0.506
	No	80 (16.2%)	87 (17.6%)	
Tumor site	Oral cavity	140 (28.3%)	165 (33.4%)	0.003**
	Pharynx	53 (10.7%)	26 (5.3%)	
	Larynx	54 (10.9%)	56 (11.3%)	
T stage	1	25 (5.1%)	10 (2.0%)	0.016*
	2	80 (16.2%)	67 (13.6%)	
	3	59 (11.9%)	75 (15.2%)	
	4	83 (16.8%)	95 (19.2%)	
N stage	0	115 (23.5%)	129 (26.3%)	0.211
	1	38 (7.8%)	47 (9.6%)	
	2	88 (18.0%)	68 (13.9%)	
	3	3 (0.6%)	2 (0.4%)	
Clinical stage	1	15 (3.0%)	5 (1.0%)	0.020*
	2	46 (9.3%)	49 (9.9%)	
	3	44 (8.9%)	65 (13.2%)	
	4	142 (28.7%)	128 (25.9%)	
Perineural invasion	Yes	71 (14.4%)	93 (18.8%)	0.109
	No	98 (19.8%)	87 (17.6%)	
	Unknown	78 (15.8%)	67 (13.6%)	
HPV status	Yes	25 (5.1%)	5 (1.0%)	0.001**
	No	33 (6.7%)	39 (7.9%)	
	Unknown	189 (38.3%)	203 (41.1%)	

* $P < 0.05$, ** $P < 0.01$.

18 T cell subpopulations and another 6 immune cells (30). The relative abundances of 24 immune cells in tumors or normal tissues of HNSCC or CESC were downloaded from <http://bioinfo.life.hust.edu.cn/ImmuCellAI#!/resource>. In addition, the relative proportions of immune cells in the tumor or normal tissues of HNSCC were also calculated by using another online immune cell analytical tool, CIBERSORTx, which supports a deconvolution algorithm to evaluate the relative proportion of immune cells in tumor tissues (31). The composition of immune cells was calculated online (<https://cibersortx.stanford.edu/>).

Analysis of Differentially Expressed Genes

The differentially expressed genes (DEG) in tumor tissues between the $\gamma\delta$ T-hi and $\gamma\delta$ T-lo groups were analyzed by R package DESeq2, and the selection criteria for DEGs were an absolute value of \log_2 FoldChange > 1 and adjusted P -value (Padj) < 0.05 . Biological process (BP) in Gene Ontology (GO) and Kyoto Gene and Genome Encyclopedia (KEGG) term

enrichment analyses were performed by R package clusterProfiler (version: 3.16.1) using the DEGs in the $\gamma\delta$ T-hi and $\gamma\delta$ T-lo group, respectively, the significance levels of enrichment results (adjusted P -values) were calculated by hypergeometric distribution. The Gene Set Enrichment Analysis (GSEA) was performed using the REACTOME database in MSigDB (version 7.1), and P -values for GSEA analyses were calculated by permutation tests. The normalized enrichment score (NES) > 1 , $P < 0.05$, and False Discovery Rates (FDR) < 0.25 were considered statistically significant in GSEA analyses.

Statistical Analyses

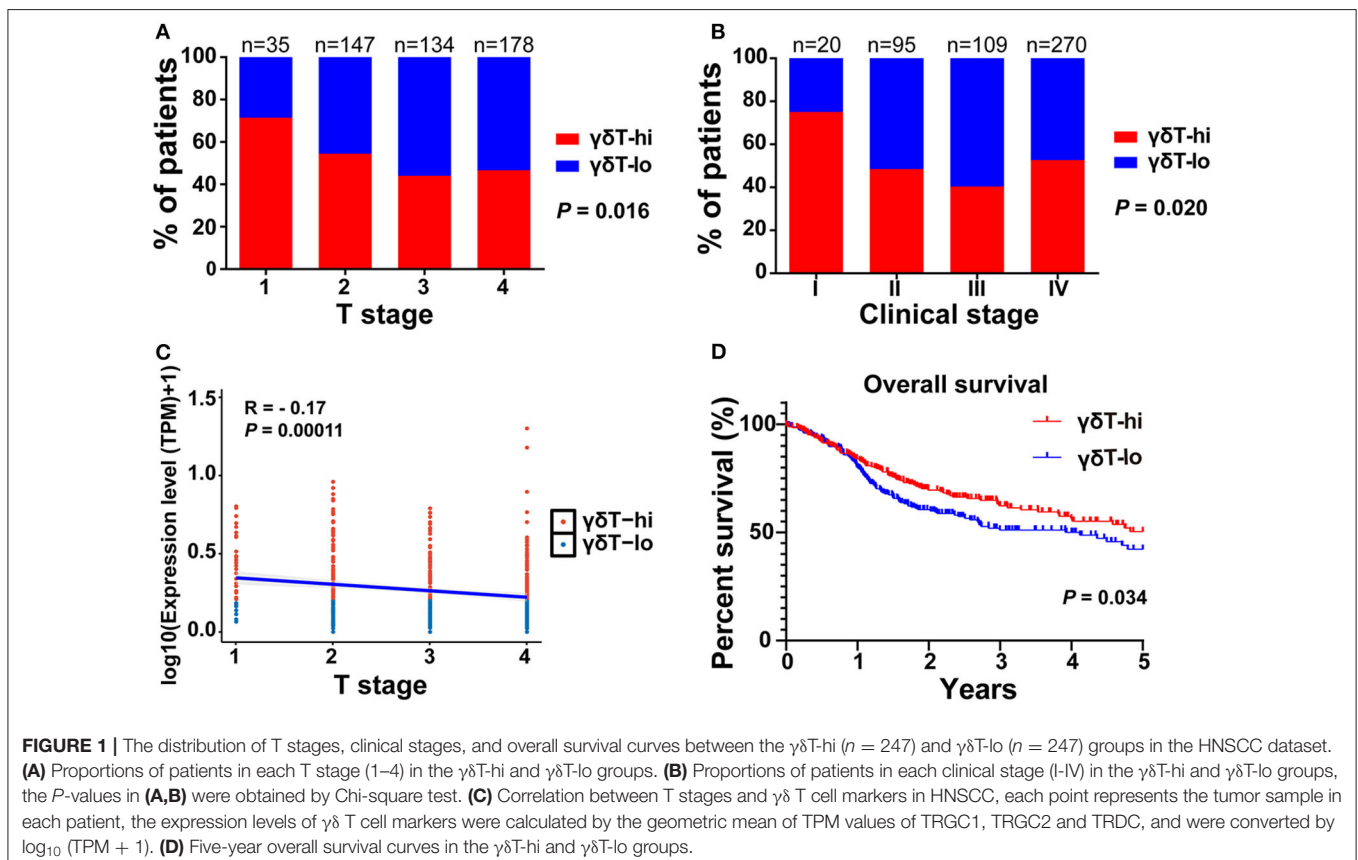
SPSS software version 25.0 was used for statistical analysis. The clinical parameters in this study included gender, age, smoking history, drinking history, tumor location, T stage, N stage, clinical stage, perineural invasion (PNI) and human papillomavirus (HPV) status. A Chi-square test was used to compare the clinical parameters between the two groups. OS was calculated and described by the Kaplan–Meier method. The difference of survival curves was tested by log-rank test. Univariate Cox proportional models were used to analyze the associations between clinical parameters and OS, and the factors with statistical significance were further included into multivariate Cox regression analysis. $P < 0.05$ was considered to be statistically significant (Wald test). GraphPad Prism version 7.0 was used to draw stacked histograms and survival curves of

$\gamma\delta$ T-hi and $\gamma\delta$ T-lo groups. ns, not significant; * $P < 0.05$; ** $P < 0.01$; *** $P < 0.001$; **** $P < 0.0001$.

RESULTS

A High Abundance of $\gamma\delta$ T Cells Is Significantly Correlated With Improved Survival of HNSCC Patients

First, we compared the clinical parameters and the OS of HNSCC patients between the $\gamma\delta$ T-hi and $\gamma\delta$ T-lo groups. The results showed that patients in the $\gamma\delta$ T-hi group accounted for a higher proportion in the T1/T2 stages (Figure 1A, Table 1) and in phase I/II clinical stages (Figure 1B, Table 1), whereas patients in the $\gamma\delta$ T-lo group were more aggregated in the T3/T4 stages and phase III/IV stages. In addition, there was a negative correlation between T stages and $\gamma\delta$ T cell marker expression levels ($R = -0.17$, $P < 0.05$, Figure 1C). The overall survival curve of the two groups showed that the survival time of the $\gamma\delta$ T-hi group was significantly prolonged ($P < 0.05$, Figure 1D). Except for the tumor site and HPV status, the clinical parameters showed no significant differences between the two groups (Table 1). However, when these factors were analyzed for univariate analysis, only $\gamma\delta$ T cell abundance, gender and PNI were significantly associated with the OS (Table 2). Furthermore, multivariate Cox regression analysis showed that only $\gamma\delta$ T cell abundance and gender were statistically significant between the



two groups (Table 2). These results showed that the abundance of $\gamma\delta$ T cells was significantly correlated with the lower clinical stages and prolonged survival of HNSCC patients. To validate whether our findings could be replicated to other types of cancer, we studied an additional squamous cell carcinoma, CESC. The results showed that similar to our findings in HNSCC, CESC patients with a higher $\gamma\delta$ T cell infiltration were positively correlated with a better OS (Supplementary Figure 1A) and the proportions of the $\gamma\delta$ T-hi group decreased in T3/4 stages, although there was no statistical significance among the T stages ($P > 0.05$, Supplementary Figure 1B).

$\gamma\delta$ T Cell Abundance Is Positively Correlated With CD4+ and CD8+ T Cell Abundance in the HNSCC Samples

Since the $\gamma\delta$ T cell abundance was positively correlated with improved survival of HNSCC patients, we next tried to explore the potential reasons for these new findings. We used the new online immune cell proportion estimation tool ImmuCellAI to analyze the abundance of 24 kinds of immune cells in the RNA-seq results of 537 samples. This tool was reported to possess a high accuracy in predicting the composition of immune cells in tumor tissues, especially T cells (30). The results showed that the $\gamma\delta$ T cell proportion in the $\gamma\delta$ T-hi group was significantly increased ($P < 0.0001$, Figure 2A), which was consistent with our grouping method. Moreover, both CD4+ T cell and CD8+ T cell abundances in the $\gamma\delta$ T-hi group increased significantly ($P < 0.0001$, Figures 2B,C). Among CD4+ T cells, T helper cells type 1 (Th1), T helper cells type 2(Th2), and follicular helper T cells (Tfh) were significantly increased in the $\gamma\delta$ T-hi group ($P < 0.0001$, Figure 2B), while the proportion of naïve CD4+ T cells and T helper cell type 17 (Th17) was lower than those in $\gamma\delta$ T-lo or normal groups (Figure 2B). However, the increase in CD4+ T cell infiltration was also accompanied by the increase of regulatory T cell abundance in the $\gamma\delta$ T-hi group (Figure 2B). In CD8+ T cells, central memory T cells, cytotoxic T cells, and exhausted T cells accumulated in the $\gamma\delta$ T-hi group, while the proportion of naïve CD8+ T cells decreased significantly, but the proportion of effector memory T cells was not increased when compared to the $\gamma\delta$ T-lo or normal groups (Figure 2C). In addition, the other cell abundances showed that the relative abundances of B cells, natural killer (NK) cells and macrophages increased significantly in the $\gamma\delta$ T-hi group, and the proportion of natural killer T (NKT) cells, monocytes and neutrophils decreased significantly (Figure 2D). To verify these results, we used another online immune cell fraction estimation method, CIBERSORTx, to calculate the relative abundance of immune cells in the HNSCC samples. The results, consistent with those of ImmuCellAI algorithm, showed that the CD8+ T cells, activated CD4+ T cells, Tfh and NK cells in the $\gamma\delta$ T-hi group were significantly increased (Supplementary Figure 2A), while the monocytes and neutrophils were decreased (Supplementary Figure 2B). It has been reported that tumor-infiltrating Th17, neutrophils, and monocytes are able to promote tumor progression (32–34), and thus the relatively low abundance of Th17 cells, neutrophils and

monocytes also contributed to the better OS in the $\gamma\delta$ T-hi group. Furthermore, M1 macrophages with an antitumor effect were increased in the TME of the $\gamma\delta$ T-hi group, while the proportion of M2 macrophages, which promote tumor development, was significantly reduced (Supplementary Figure 2B). Furthermore, we have found a similar immune cell distribution pattern between the $\gamma\delta$ T-hi and $\gamma\delta$ T-lo groups in the CESC dataset calculated by ImmuCellAI algorithm (Supplementary Figures 1C–F), indicating the immune cell infiltration may be affected by $\gamma\delta$ T cells in the TME across different types of cancer.

Genes Related to T Cell Effector Functions and Chemokine Production Are Highly Expressed in the $\gamma\delta$ T-hi Group

We further analyzed the differential genes between $\gamma\delta$ T-hi and $\gamma\delta$ T-lo groups by using R package DESeq2. As shown in the Figures 3A,B, a total of 1,113 genes were upregulated and 329 genes were down-regulated in the $\gamma\delta$ T-hi group ($|\log_2\text{FoldChange}| > 1$, $\text{Padj} < 0.05$, Supplementary Table 1). Among these DEGs, genes encoding CD3 (CD3E/CD3G/CD3D), and genes related to Th1 cells (CD4/TBX21), CD8+ T cells (CD8A/CD8B), B cells (CD19/MS4A1), and NK cells (NCR1/NKG7) were significantly upregulated (Figure 3A), which was in line with the increased proportion of Th1/CD8+ T cells/B cells/NK cells in the $\gamma\delta$ T-hi group. In contrast, the gene KRT1 related to keratinocytes, the tumor marker AFP (alpha-fetoprotein), and ARG1 (encoding arginase1) related to inhibiting CD8+ T cell function were upregulated in the $\gamma\delta$ T-lo group (Figure 3B). NKG2D, the surface marker of activated cytotoxic $\gamma\delta$ T cells, and Hobit, the transcription factor that enhance the cytotoxicity of $\gamma\delta$ T cells (35), were both upregulated in the $\gamma\delta$ T-hi group compared to those in the $\gamma\delta$ T-lo or normal group (Figure 3C). At the same time, the expression level of cytokines and granzymes (IFNG/GZMA/GZMB/GNLY) were also significantly increased in the $\gamma\delta$ T-hi group (Figure 3D). These results revealed the enhanced effector functions of tumor-infiltrating T cells of the $\gamma\delta$ T-hi group. Previous studies have reported that $\gamma\delta$ T cells could release chemokines CCL5 and CXCL9 to attract other T cells to fight against pathogens or tumors (26, 36). In the $\gamma\delta$ T-hi group, we found that these two chemokines were also significantly upregulated, and they are reported to be essential for the recruitment of CD8+ T cells to the TME for tumor cell killing (Figure 3E). Therefore, $\gamma\delta$ T cells may also recruit CD8+ T cells via chemokine release.

Gene Sets and Cell Pathways Related to T Cell Activation, Proliferation, Chemokine Production and Cytotoxicity Are Enriched in the $\gamma\delta$ T-hi Group

We then performed GO and KEGG term enrichment on the DEGs in the $\gamma\delta$ T-hi group and the $\gamma\delta$ T-lo group, respectively. The results showed that the genes upregulated in the $\gamma\delta$ T-hi group enriched the functions related to T cell activation, proliferation, differentiation, cytokine production, and cell-cell adhesion in the GO biological process (Figure 4A). In the KEGG results, the $\gamma\delta$ T-hi group was enriched for terms including cytokine-cytokine

TABLE 2 | Univariate and multivariate survival analysis of HNSCC patients in TCGA database.

Factor	P-value (Univariate)	Hazard ratio (Multivariate)	P-value (Multivariate)
$\gamma\delta$ T cell abundance	0.047*	0.734	0.036*
gender	0.023*	0.702	0.023*
age	0.295		
Smoking history	0.906		
Alcohol history	1.000		
tumor site	0.153		
T stage	0.297		
N stage	0.360		
Clinical stage	0.962		
Perineural invasion	<0.001*	1.066	0.058
HPV status	0.212		

* $P < 0.05$.

receptor interaction, chemokine signaling pathway, T cell and B cell receptor pathway, Th1 and Th2 cell differentiation, and others (Figure 4B). Furthermore, it was noted that chemokine bind chemokine receptors, complement cascade, interferon- γ pathway, and MHC-II antigen presentation were significantly enriched in the $\gamma\delta$ T-hi group through the GSEA analysis ($P < 0.05$, FDR < 0.25 , Figure 4C). The genes that participate in the complement pathway and antigen presentation, including C7/CR2/HLA-DRA, were also found in the $\gamma\delta$ T-hi group (Figures 3A,B), indicating that the complement cascade and antigen presentation were also involved in the $\gamma\delta$ T cell-mediated immune response. In contrast, only biological processes such as cell keratinization and hormone metabolism were enriched in the $\gamma\delta$ T-lo group (Figure 4D). It was reported that $\gamma\delta$ T cells could also serve as antigen-presenting cells to activate conventional T cells in infectious disease or the TME (37), our results, consistent with these previous studies, showed that $\gamma\delta$ T cells may exert antitumor responses by activating and recruiting effector T cells or NK cells to the TME and through MHC-II antigen presentation, but the exact mechanism is still unknown.

The Abundance of $\gamma\delta$ T Cells Is Positively Associated With the Expression of Butyrophilin Family Proteins in Tumor Cells

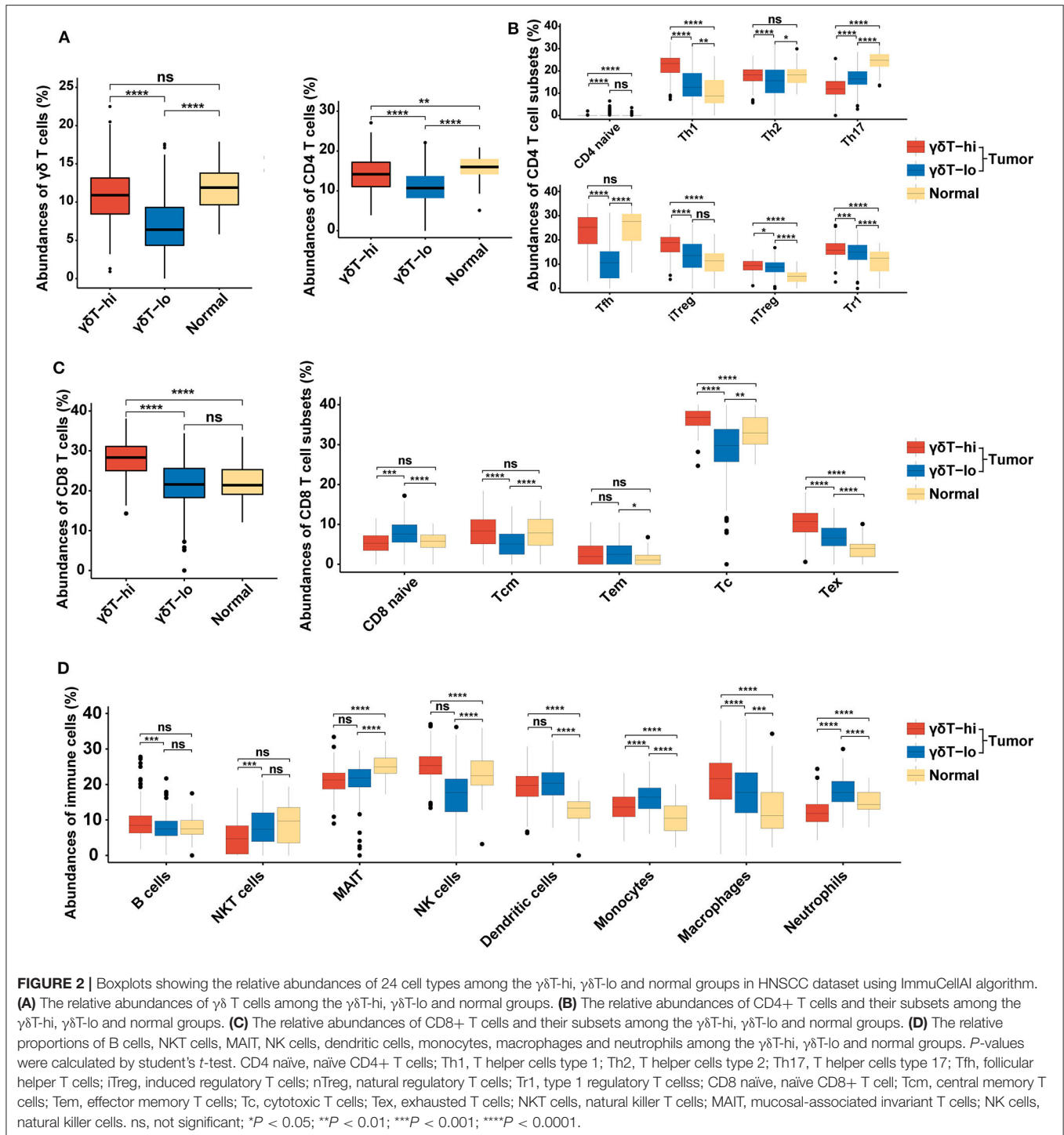
We have explored the possible antitumor mechanism of $\gamma\delta$ T cells in HNSCC, but the factors that contribute to the increase in $\gamma\delta$ T cells in the TME are still unclear. Thus, we explored the expression levels of BTNs and NKG2DLs among the three groups and performed the linear correlation analysis between the expression levels of BTNs or NKG2DLs and the $\gamma\delta$ T cell markers. We found that the expression levels of BTN2A1/BTN3A1/BTN3A2/BTN3A3 in the $\gamma\delta$ T-hi group were significantly higher than those in the $\gamma\delta$ T-lo group or normal group ($P < 0.0001$), and the expression levels of BTNs in the normal control group were the lowest (Figure 5A). Through linear regression analysis, we found that there was a relatively strong correlation between BTN3A1/BTN3A2/BTN3A3 and the $\gamma\delta$ T cell markers, while the correlation between BTN2A1 and the $\gamma\delta$ T cell markers was relatively weak (Figure 5C). Furthermore,

the results showed that only MICB expression in the $\gamma\delta$ T-hi group was significantly higher than that in the $\gamma\delta$ T-lo or normal groups, while MICA expression was not significantly higher than that in the $\gamma\delta$ T-lo group (Figure 5B). Linear regression analysis showed that MICB expression had moderate correlation with $\gamma\delta$ T cell markers, while MICA showed nearly no correlation (Figure 5C). In contrast, the expression of ULBP family proteins in $\gamma\delta$ T-hi was lower than that in the $\gamma\delta$ T-lo group, suggesting that activation of the $\gamma\delta$ T cells in HNSCC might not be related to the ULBP family proteins (Supplementary Figure 3A). However, when we dichotomized the HNSCC cohort based on the median expression levels of BTN3A1/BTN3A2/BTN3A3/BTN2A1, we found that although there was no statistical significance between the high and low groups, the patients with higher expression levels of the BTN family proteins showed better overall survival than patients whose expression levels were lower than the median expression levels ($P > 0.05$, Supplementary Figure 3B).

DISCUSSION

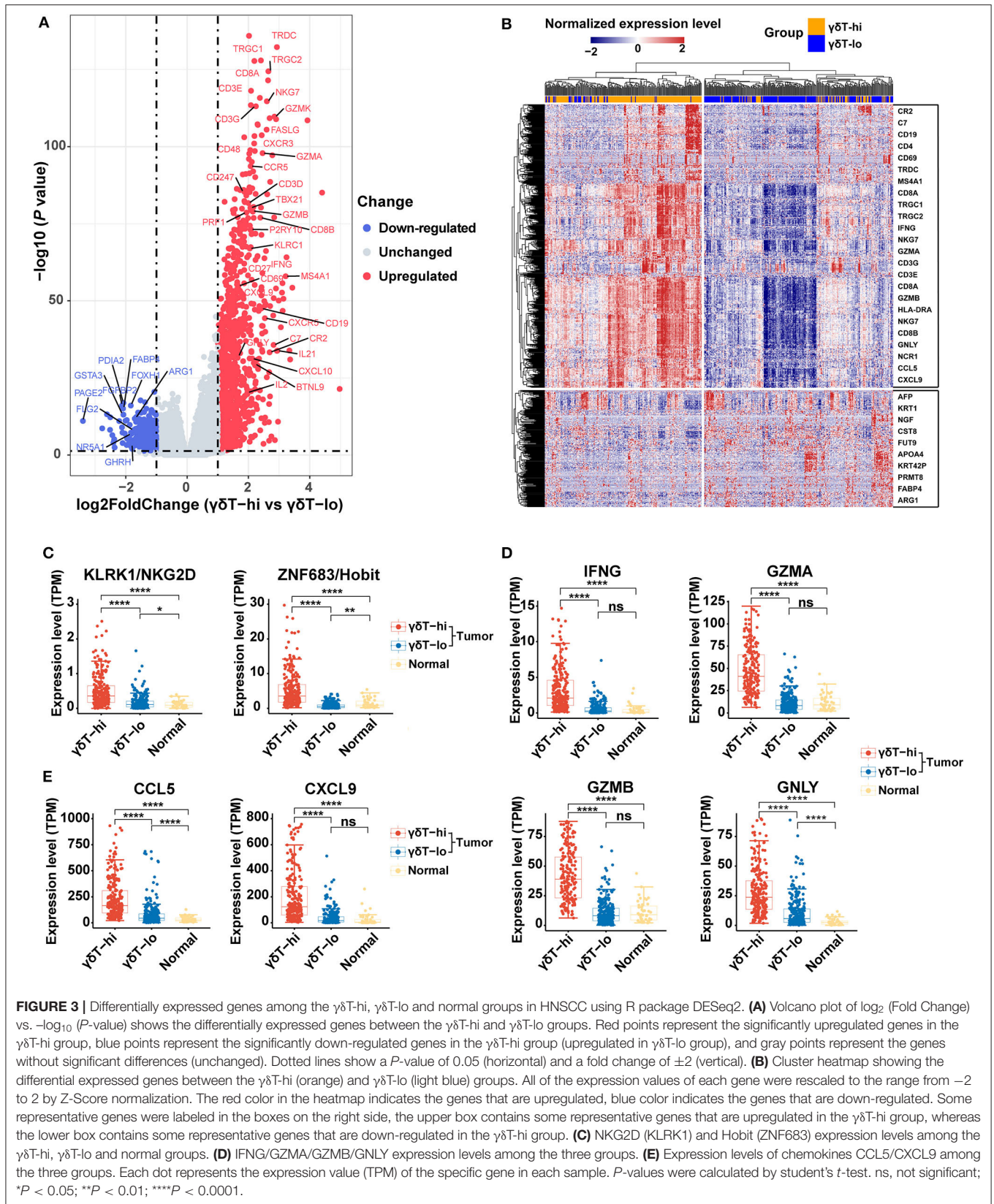
In the present study, we used TCGA dataset to demonstrate that the high abundance of $\gamma\delta$ T cells in HNSCC was positively associated with an improved prognosis of patients, possibly due to the enhanced antitumor effect of $\gamma\delta$ T cells and the recruitment of CD8+ T cells to the TME. Finally, we found that the increased $\gamma\delta$ T cell abundance in the TME was associated with upregulation of BTN family proteins and the NKG2D ligand MICB in tumor cells, indicating that the activation of $\gamma\delta$ T cells may be associated with BTN family proteins and MICB.

Tumor-infiltrating lymphocytes play a vital role in the control of tumor progression, with different clinical effects (38). Similar to $\alpha\beta$ T cells, $\gamma\delta$ T cells are also found in various types of human tumors. Both V δ 1 T and V δ 2 T cells have been found in various epithelial tumors, such as lung cancer, renal cancer, melanoma, and colorectal cancer (12). By applying the CIBERSORT analysis in a pan-cancer analysis of over 18,000 human tumors in TCGA data, $\gamma\delta$ T cells were found to be the most favorable prognostic populations among all types of tumor-infiltrating leukocytes across all types of tumors (39). However, whether $\gamma\delta$ T cells



exert antitumor or protumor effects in the TME has not been validated. $V\delta 2$ T cells activated by non-peptide phosphoantigens *in vitro* have been proven to inhibit tumor growth both *in vitro* and *in vivo* (40, 41). Currently, the results of phase I clinical trials on advanced lung cancer, renal cancer and melanoma have revealed that adoptive $V\delta 2$ T cell transfer therapies have shown certain antitumor effects (42). However, other studies have

reported that $V\delta 2$ T cells can also promote tumor progression (43). Under specific stimulation, $V\delta 2$ T cells can be differentiated into subsets endowed with Th17 or Treg characteristics, exerting protumor and immunosuppressive effects by producing IL-17 and IL-10, respectively (44). In addition, $V\delta 1$ T cells have also been found to have dual effects in tumor immunity. In patients with hepatocellular carcinoma (45) and gastric cancer (46),



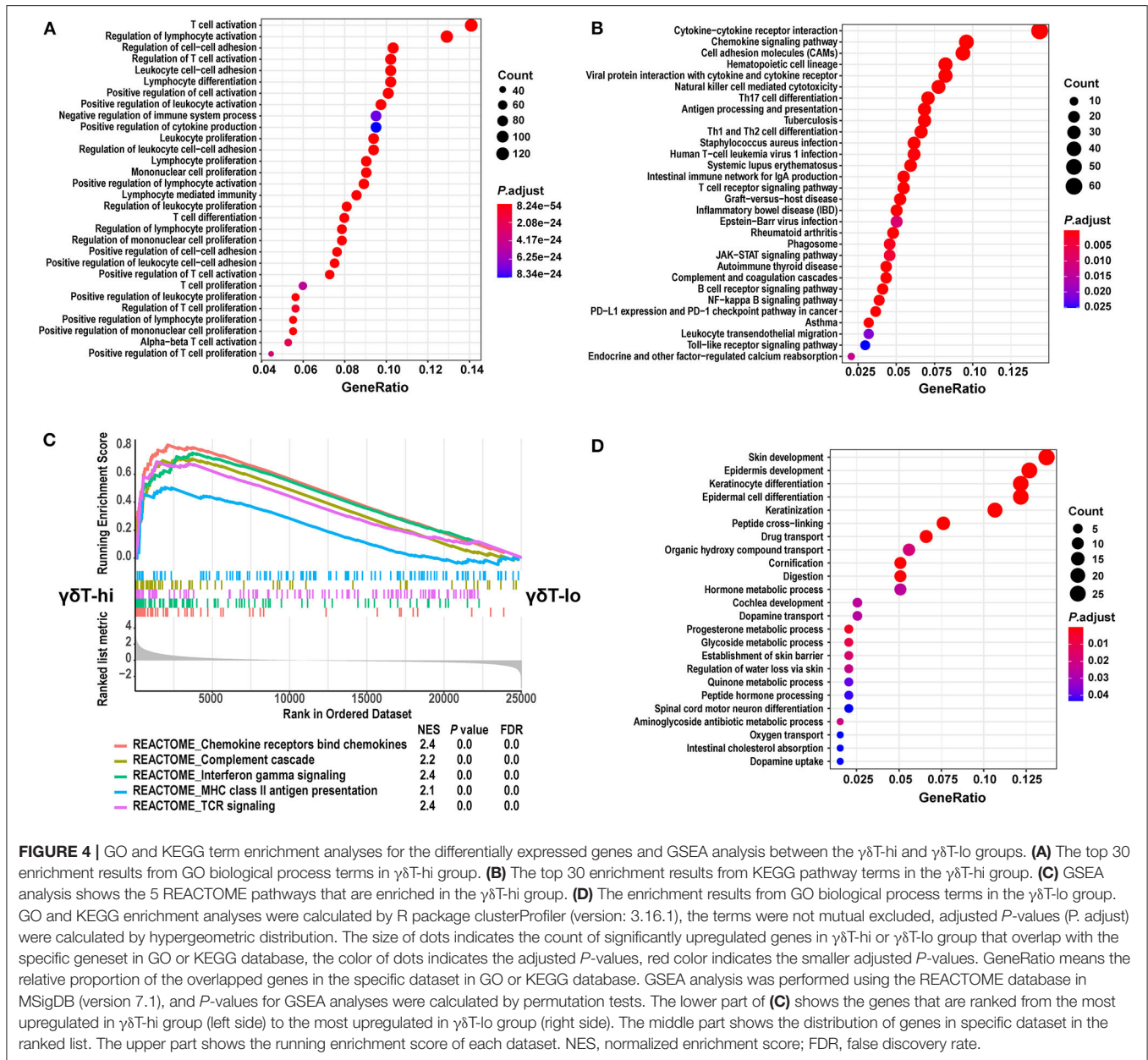
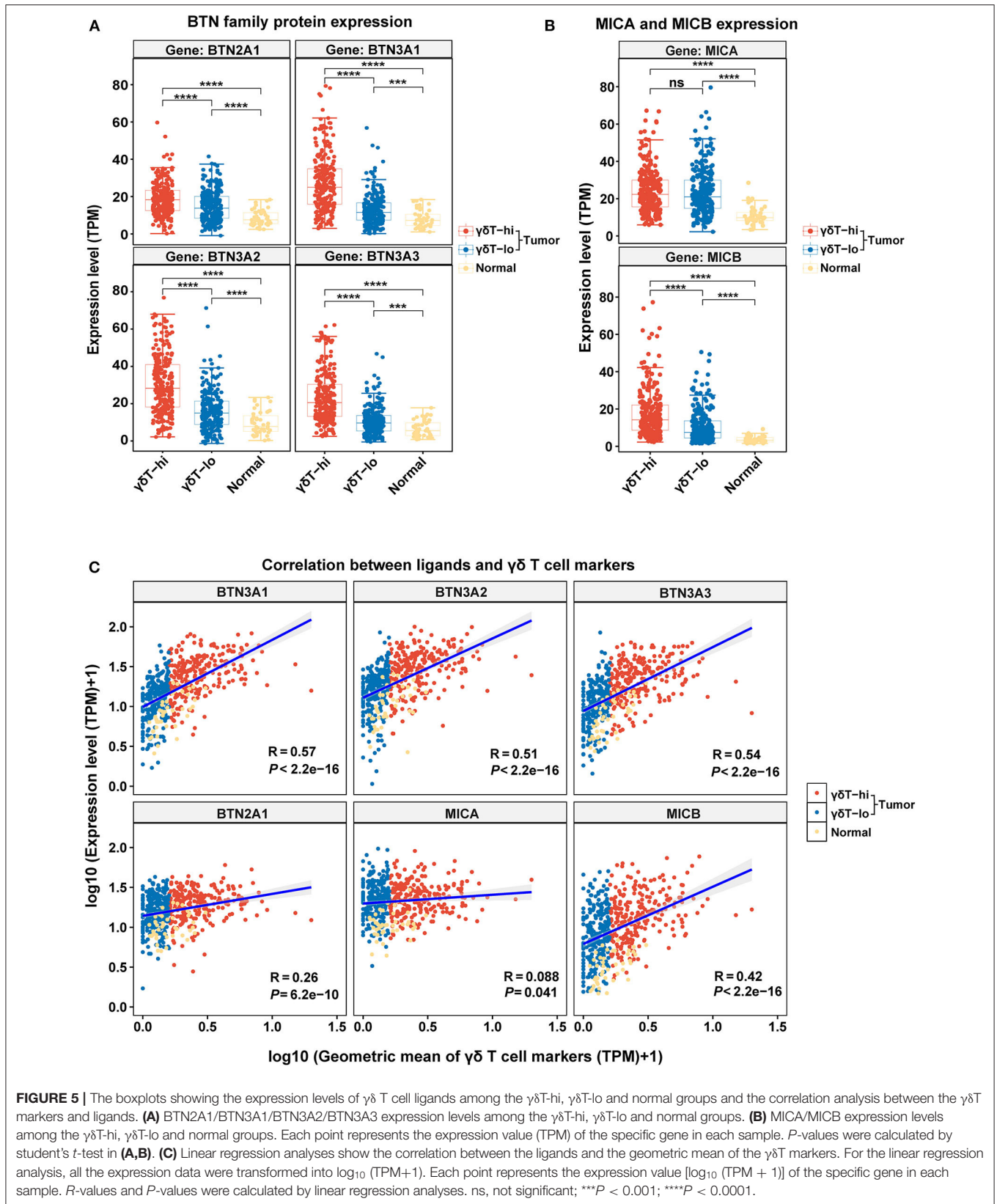


FIGURE 4 | GO and KEGG term enrichment analyses for the differentially expressed genes and GSEA analysis between the $\gamma\delta$ T-hi and $\gamma\delta$ T-lo groups. **(A)** The top 30 enrichment results from GO biological process terms in $\gamma\delta$ T-hi group. **(B)** The top 30 enrichment results from KEGG pathway terms in the $\gamma\delta$ T-hi group. **(C)** GSEA analysis shows the 5 REACTOME pathways that are enriched in the $\gamma\delta$ T-hi group. **(D)** The enrichment results from GO biological process terms in the $\gamma\delta$ T-lo group. GO and KEGG enrichment analyses were calculated by R package clusterProfiler (version: 3.16.1), the terms were not mutual excluded, adjusted *P*-values (*P*. adjust) were calculated by hypergeometric distribution. The size of dots indicates the count of significantly upregulated genes in $\gamma\delta$ T-hi or $\gamma\delta$ T-lo group that overlap with the specific geneset in GO or KEGG database, the color of dots indicates the adjusted *P*-values, red color indicates the smaller adjusted *P*-values. GeneRatio means the relative proportion of the overlapped genes in the specific dataset in GO or KEGG database. GSEA analysis was performed using the REACTOME database in MSigDB (version 7.1), and *P*-values for GSEA analyses were calculated by permutation tests. The lower part of **(C)** shows the genes that are ranked from the most upregulated in $\gamma\delta$ T-hi group (left side) to the most upregulated in $\gamma\delta$ T-lo group (right side). The middle part shows the distribution of genes in specific dataset in the ranked list. The upper part shows the running enrichment score of each dataset. NES, normalized enrichment score; FDR, false discovery rate.

a high infiltration of $\gamma\delta$ 1 T cells is associated with a longer survival time, but in patients with breast cancer (47) or colorectal cancer (13), high infiltration of $\gamma\delta$ T cells is associated with poor prognosis. Our results have showed that patients with higher $\gamma\delta$ T cell proportions were correlated with lower T stages, and a longer overall survival of HNSCC patients both in univariate and multivariate analyses, suggesting that $\gamma\delta$ T cells may be involved in the antitumor immunity in HNSCC. However, a previous study has shown that there was no correlation between the proportions of $\gamma\delta$ T cells and tumor stages in HNSCC patients (14), which is seemingly paradoxical with our results. The possible explanation is that the previous study only compared the $\gamma\delta$ T cell abundance in peripheral blood, whereas $\gamma\delta$ T cells

in the TME were not analyzed. The composition of lymphocytes in the peripheral blood and the TME may be different, and due to the lack of RNA-seq data from the peripheral blood in HNSCC patients of TCGA dataset, it is not possible to explore whether $\gamma\delta$ T cells in peripheral blood reflect those in the TME.

$\gamma\delta$ T cells are considered as a bridge between innate and adaptive immune responses. Apart from direct tumor cell killing, $\gamma\delta$ T cells interact with other innate and adaptive immune cells in the TME to exert indirect antitumor responses. IFN- γ secreted by $\gamma\delta$ T cells promotes the upregulation of MHC-I molecules on tumor cells and positively regulates the antitumor function of CD8+ T cells (48). In addition, $\gamma\delta$ T cells activate NK cells through the CD137/CD137L axis,



promoting cytotoxicity in solid tumors (49). In the presence of P-Ags and interleukin 21, V δ 2 T cells can also express Tfh cell-related markers, such as ICOS, CD40L and CXCR5 and these Tfh-like $\gamma\delta$ T cells ($\gamma\delta$ Tfh) secrete cytokines, such as IL-4 and CXCL13, to increase antibody production of B cells (48). In addition, $\gamma\delta$ T cells also serve as antigen presenting cells to activate CD8+ T cells and Th1 cells (37). Consistent with the previous research, our study found that the high abundance of $\gamma\delta$ T cells was accompanied by the increase in CD8+ T cells, Th1 cells, Tfh cells, B cells, and other cell subsets. Moreover, through gene ontology and pathway enrichment analyses, it was indicated that $\gamma\delta$ T cells might be involved in the activation of the IFN- γ signaling pathway, antigen presentation, chemokine secretion and other biological processes.

The unexpected discoveries in our study are that regulatory T cells, which are known as negative regulators of the immune response and contribute to tumor progression, accumulated in the $\gamma\delta$ T-hi group. Previous studies have revealed that higher Treg abundance was associated with shorter overall survival in renal cancer, breast cancer or melanoma (50), while high infiltration of Foxp3+ Treg cells in HNSCC was associated with an improved overall survival (51), and studies have revealed that higher CD8+ T cell or NK cell infiltration was usually accompanied by higher infiltration of Tregs in HNSCC (51); therefore it is hypothesized that Tregs are trafficked into the TME after CD8+ T and NK cells as a negative feedback to prevent the excessive inflammation mediated by CD8+ T cells and NK cells. In addition, we also discovered that the proportion of exhausted CD8+ T cells accumulated but that NKT cells were decreased in the $\gamma\delta$ T-hi group, which was seemingly paradoxical with our results. Although it is known that T cell exhaustion is a state in which antigen-specific CD8+ T cells undergo a progressive and hierarchical loss of effector functions during chronic antigen stimulation in the tumor microenvironment (52), this process does not occur in other bystander CD8+ T cells (53), and recent studies have also revealed that it is the exhausted T cells that exert the antitumor effect in an antigen-specific manner (53); previous studies have also discovered this phenomenon that HNSCC patients with higher expression of exhausted markers, including PDCD1, TIM3, and CD39, were associated with a better OS (54). Therefore, the more antigen-specific T cells that enter the TME, the greater chance they may terminally differentiate into exhausted T cells. For NKT cell, although it is an innate-like lymphocyte with invariant TCR that exerts potent antitumor immunity (55), the activation and expansion of NKT cells requires the presentation of α -galactosylceramide (α -GalCer) (56), a specific glycolipid antigen that is almost absent in the TME, and thus the expansion capacity of NKT cells in the TME is restrained. Therefore, compared to other T cell subsets that proliferate rapidly in the TME in the $\gamma\delta$ T-hi group, including CD8+ T cells, CD4+ T cells or $\gamma\delta$ T cells, the number of NKT cells remains unchanged, resulting in the relatively lower proportions compared to the $\gamma\delta$ T-lo group.

As a novel group of type I transmembrane proteins of the immunoglobulin superfamily, the butyrophilin family of

proteins shares a high homology with the B7 family proteins of the extracellular domains, suggesting that BTNs may also possess immunoregulatory functions (57). Among the BTN families, BTN1A1 and BTN2A2 have been reported to inhibit the activation and immune response of conventional T cells (58, 59). However, BTN3A1, along with BTN3A2 and BTN3A3, was required for P-Ag presentation and activation of V δ 2 T cells (18, 19). In addition, recent studies have revealed that BTN2A1 was another ligand that cooperated with BTN3A1 to activate V δ 2 T cells (20, 60). Studies have shown that a TP53 gene mutation would lead to the activation of the mevalonate pathway in cancer cells, resulting in the accumulation of isopentenyl pyrophosphate (IPP) and its isomer dimethylallyl pyrophosphate (DMAPP) in tumor cells (61). These metabolites would be taken up by BTNs and presented to V δ 2 T cells, leading to the activation of $\gamma\delta$ T cells and an enhanced antitumor immune response (62, 63). Studies have shown that through binding to P-Ags presented by BTN3A1 and BTN2A1 on infected or malignant cells, $\gamma\delta$ T cells could be activated, proliferate rapidly, and induce anti-infection or antitumor responses through IFN- γ production (20). Notably, it has been demonstrated that the B30.2 domain of BTN3As can bind P-Ag and drive the activation of V δ 2 T cells through conformational changes of the extracellular domains (64, 65), and periplakin and RhoB are the key proteins that play important roles in spatial rearrangement of BTN3As following intracellular P-Ag sensing (66–68). But how then do P-Ag enter the cells to initiate $\gamma\delta$ T cell activation following binding to cytosolic B30.2 is needed to be clarified. Recent studies have found that a higher expression of BTN3A2 in ovarian cancer or triple negative breast cancer is positively correlated with an increased T cell infiltration and a better prognosis (23, 69). Our results, in line with previous studies, showed that $\gamma\delta$ T cells in the TME might be activated in a butyrophilin-dependent manner, and mediated an antitumor response against HNSCC.

Apart from the interaction of the BTN family proteins and TCR $\gamma\delta$, the binding of NKG2D with NKG2DLs is the costimulatory signaling pathway that activates $\gamma\delta$ T cells. It was reported that tumor cells expressing NKG2DLs (both MIC proteins and ULBP proteins) were more susceptible to $\gamma\delta$ T cell-mediated lysis (70). However, although the expression level of NKG2D was much higher in the $\gamma\delta$ T-hi group, only MICB expression was upregulated in the $\gamma\delta$ T-hi group among the NKG2DLs, while MICA expression was not upregulated, with the ULBP family proteins showing the opposite results. The possible explanation for these results is that the activation of $\gamma\delta$ T cells is not primarily through the NKG2DL-NKG2D pathway, and another possible explanation is that apart from the NKG2DLs expressed on tumor cells, the soluble NKG2DLs can also suppress the antitumor response of $\gamma\delta$ T cells (71). The exact mechanisms of how NKG2DLs activate $\gamma\delta$ T cells in head and neck cancer still need further exploration. Collectively, our results showed that $\gamma\delta$ T cells might be activated and exert antitumor effects mainly through the recognition of BTN family proteins, which might be promising targets for $\gamma\delta$ T-cell mediated immunotherapy.

In conclusion, our results showed that the abundance of $\gamma\delta$ T cells in the tumors was positively associated with the improvement of prognosis in HNSCC patients. This antitumor effect might be attributed to the enhancement of $\gamma\delta$ T cell-mediated cytotoxicity and the recruitment and activation of other antitumor lymphocytes. BTN2A1 and BTN3As might be the direct ligands that activate $\gamma\delta$ T cells in head and neck cancers. Our results provide a new perspective of the HNSCC microenvironment, and provide potential targets for immunotherapy of HNSCC, which deserve further exploration.

DATA AVAILABILITY STATEMENT

All datasets generated for this study are included in the article/**Supplementary Material**.

AUTHOR CONTRIBUTIONS

ZW contributed to conception and design of the study. HL contributed to the design of the study and acquisition and analysis of the data. WD, JG, and DW contributed to the analysis and interpretation of the data. SW, LY, DL, WX, LW, and JF contributed to the interpretation of the data. HL, WD, and JG wrote the first draft of the manuscript. DW, SW, LY, DL, and WX wrote sections of the manuscript. All authors contributed to manuscript revision, read, and approved the submitted version.

FUNDING

This work was supported by the National Natural Science Foundations of China (Nos. 81972532, 81772896, and 81630025) and the Science and Technology Planning Project of Guangzhou City of China (No. 2017004020102).

REFERENCES

- Peres MA, Macpherson LMD, Weyant RJ, Daly B, Venturini R, Mathur MR, et al. Oral diseases: a global public health challenge. *Lancet*. (2019) 394:249–60. doi: 10.1016/S0140-6736(19)31146-8
- Chow LQM. Head and neck cancer. *N Engl J Med*. (2020) 382:60–72. doi: 10.1056/NEJMra1715715
- Chi AC, Day TA, Neville BW. Oral cavity and oropharyngeal squamous cell carcinoma—an update. *CA Cancer J Clin*. (2015) 65:401–21. doi: 10.3322/caac.21293
- Ferris RL, Blumenschein G Jr, Fayette J, Guigay J, Colevas AD, et al. Nivolumab for recurrent squamous-cell carcinoma of the head and neck. *N Engl J Med*. (2016) 375:1856–67. doi: 10.1056/NEJMoa1602252
- Seiwert TY, Burtress B, Mehra R, Weiss J, Berger R, Eder JP, et al. Safety and clinical activity of pembrolizumab for treatment of recurrent or metastatic squamous cell carcinoma of the head and neck (KEYNOTE-012): an open-label, multicentre, phase 1b trial. *Lancet Oncol*. (2016) 17:956–65. doi: 10.1016/S1470-2045(16)30066-3

SUPPLEMENTARY MATERIAL

The Supplementary Material for this article can be found online at: <https://www.frontiersin.org/articles/10.3389/fimmu.2020.573920/full#supplementary-material>

Supplementary Figure 1 | The distribution of T stages and overall survival curves between $\gamma\delta$ T-hi ($n = 139$) and $\gamma\delta$ T-lo ($n = 139$) groups and the immune cell abundances among the $\gamma\delta$ T-hi, $\gamma\delta$ T-lo and normal groups ($n = 3$) in the CESC dataset. **(A)** Five-year overall survival curves between the $\gamma\delta$ T-hi and $\gamma\delta$ T-lo groups. **(B)** The proportions of patients in each T stage (1–4) in the $\gamma\delta$ T-hi and $\gamma\delta$ T-lo groups. **(C)** The relative abundances of $\gamma\delta$ T cells among the $\gamma\delta$ T-hi, $\gamma\delta$ T-lo and normal groups calculated by ImmuCellAI algorithm. **(D)** The relative abundances of CD4+ T cells and their subsets among the $\gamma\delta$ T-hi, $\gamma\delta$ T-lo and normal groups calculated by ImmuCellAI algorithm. **(E)** The relative abundances of CD8+ T cells and their subsets among the $\gamma\delta$ T-hi, $\gamma\delta$ T-lo and normal groups calculated by ImmuCellAI algorithm. **(F)** The relative abundances of B cells, NKT cells, MAIT, NK cells, dendritic cells, monocytes, macrophages and neutrophils among the $\gamma\delta$ T-hi, $\gamma\delta$ T-lo and normal groups calculated by ImmuCellAI algorithm. *P*-values were calculated by student's *t*-test. CD4 naïve, naïve CD4+ T cells; Th1, T helper cells type 1; Th2, T helper cells type 2; Th17, T helper cells type 17; Tfh, follicular helper T cells; iTreg, induced regulatory T cells; nTreg, natural regulatory T cells; Tr1, type 1 regulatory T cells; CD8 naïve, naïve CD8+ T cell; Tcm, central memory T cells; Tem, effector memory T cells; Tc, cytotoxic T cells; Tex, exhausted T cells; NKT cells, natural killer T cells; MAIT, mucosal-associated invariant T cells; NK cells, natural killer cells. ns, not significant; **P* < 0.05; ***P* < 0.01; ****P* < 0.001; *****P* < 0.0001.

Supplementary Figure 2 | Relative abundance of cell types among the $\gamma\delta$ T-hi, $\gamma\delta$ T-lo and normal groups in HNSCC by using CIBERSORTx. **(A)** The proportions of lymphocyte subsets (B cells, T cells and NK cells) among the $\gamma\delta$ T-hi, $\gamma\delta$ T-lo and normal groups. **(B)** The relative proportions of myeloid cell subsets (monocytes, macrophages dendritic cells, mast cells, eosinophils and neutrophils) among the $\gamma\delta$ T-hi, $\gamma\delta$ T-lo and normal groups. *P*-values were calculated by student's *t*-test. ns, not significant; ***P* < 0.01; ****P* < 0.001; *****P* < 0.0001.

Supplementary Figure 3 | The expression levels of ULBP family proteins among the $\gamma\delta$ T-hi, $\gamma\delta$ T-lo and normal groups, and the association between BTN family proteins and 5-year OS. **(A)** The expression levels of ULBP1/ULBP2/ULBP3/RAET1E/RAET1G/RAET1L among the $\gamma\delta$ T-hi, $\gamma\delta$ T-lo and normal groups. Each point represents the expression value (TPM) of the specific gene in each sample. *P* values were calculated by student's *t*-test. **(B)** HNSCC patients were dichotomized into high and low group based on the median expression of BTN3A1/BTN3A2/BTN3A3/BTN2A1, and the OS curves were drawn for the high and low group, respectively. ns, not significant; ***P* < 0.01; ****P* < 0.001; *****P* < 0.0001.

- Silva-Santos B, Mensurado S, Coffelt SB. gammadelta T cells: pleiotropic immune effectors with therapeutic potential in cancer. *Nat Rev Cancer*. (2019) 19:392–404. doi: 10.1038/s41568-019-0153-5
- Nielsen MM, Witherden DA, Havran WL. gammadelta T cells in homeostasis and host defence of epithelial barrier tissues. *Nat Rev Immunol*. (2017) 17:733–45. doi: 10.1038/nri.2017.101
- Zhao Y, Lin L, Xiao Z, Li M, Wu X, Li W, et al. Protective role of gammadelta t cells in different pathogen infections and its potential clinical application. *J Immunol Res*. (2018) 2018:5081634. doi: 10.1155/2018/5081634
- Tanaka Y, Morita CT, Tanaka Y, Nieves E, Brenner MB, Bloom BR. Natural and synthetic non-peptide antigens recognized by human gamma delta T cells. *Nature*. (1995) 375:155–8. doi: 10.1038/375155a0
- Poggi A, Venturino C, Catellani S, Clavio M, Miglino M, Gobbi M, et al. Vdelta1 T lymphocytes from B-CLL patients recognize ULBP3 expressed on leukemic B cells and up-regulated by trans-retinoic acid. *Cancer Res*. (2004) 64:9172–9. doi: 10.1158/0008-5472.CAN-04-2417
- Gooden MJ, de Bock GH, Leffers N, Daemen T, Nijman HW. The prognostic influence of tumour-infiltrating lymphocytes in cancer: a systematic review with meta-analysis. *Br J Cancer*. (2011) 105:93–103. doi: 10.1038/bjc.2011.189

12. Paul S, Lal G. Regulatory and effector functions of gamma-delta ($\gamma\delta$) T cells and their therapeutic potential in adoptive cellular therapy for cancer. *Int J Cancer*. (2016) 139:976–85. doi: 10.1002/ijc.30109
13. Wu P, Wu D, Ni C, Ye J, Chen W, Hu G, et al. $\gamma\delta$ T17 cells promote the accumulation and expansion of myeloid-derived suppressor cells in human colorectal cancer. *Immunity*. (2014) 40:785–800. doi: 10.1016/j.immuni.2014.03.013
14. Bas M, Bier H, Schirlau K, Friebe-Hoffmann U, Scheckenbach K, Balz V, et al. Gamma-delta T-cells in patients with squamous cell carcinoma of the head and neck. *Oral Oncol*. (2006) 42:691–7. doi: 10.1016/j.oraloncology.2005.11.008
15. Vermijlen D, Gatti D, Kouzeli A, Rus T, Eberl M. gammadelta T cell responses: how many ligands will it take till we know? *Semin Cell Dev Biol*. (2018) 84:75–86. doi: 10.1016/j.semdb.2017.10.009
16. Blazquez JL, Benyamine A, Pasero C, Olive D. New insights into the regulation of gammadelta T cells by BTN3A and other BTN/BTNL in tumor immunity. *Front Immunol*. (2018) 9:1601. doi: 10.3389/fimmu.2018.01601
17. Abeler-Dorner L, Swamy M, Williams G, Hayday AC, Bas A. Butyrophilins: an emerging family of immune regulators. *Trends Immunol*. (2012) 33:34–41. doi: 10.1016/j.it.2011.09.007
18. Vavassori S, Kumar A, Wan GS, Ramanjaneyulu GS, Cavallari M, El Daker S, et al. Butyrophilin 3A1 binds phosphorylated antigens and stimulates human gammadelta T cells. *Nat Immunol*. (2013) 14:908–16. doi: 10.1038/ni.2665
19. Vantourout P, Laing A, Woodward MJ, Zlatareva I, Apolonia L, Jones AW, et al. Heteromeric interactions regulate butyrophilin (BTN) and BTN-like molecules governing gammadelta T cell biology. *Proc Natl Acad Sci USA*. (2018) 115:1039–44. doi: 10.1073/pnas.1701237115
20. Rigau M, Ostrouska S, Fulford TS, Johnson DN, Woods K, Ruan Z, et al. Butyrophilin 2A1 is essential for phosphoantigen reactivity by gammadelta T cells. *Science*. (2020) 367:aay5516. doi: 10.1126/science.aay5516
21. Decaup E, Duault C, Bezombes C, Poupot M, Savina A, Olive D, et al. Phosphoantigens and butyrophilin 3A1 induce similar intracellular activation signaling in human TCRV γ 9+ $\gamma\delta$ T lymphocytes. *Immunol Lett*. (2014) 161:133–7. doi: 10.1016/j.imlet.2014.05.011
22. Benyamine A, Loncle C, Foucher E, Blazquez JL, Castanier C, Chrétien AS, et al. BTN3A is a prognosis marker and a promising target for V γ 9V δ 2 T cells based-immunotherapy in pancreatic ductal adenocarcinoma (PDAC). *Oncotarget*. (2017) 7:e1372080. doi: 10.1080/2162402X.2017.1372080
23. Cai P, Lu Z, Wu J, Qin X, Wang Z, Zhang Z, et al. BTN3A2 serves as a prognostic marker and favors immune infiltration in triple-negative breast cancer. *J Cell Biochem*. (2020) 121:2643–54. doi: 10.1002/jcb.29485
24. Zhu M, Yan C, Ren C, Huang X, Zhu X, Gu H, et al. Exome array analysis identifies variants in SPOCD1 and BTN3A2 that affect risk for gastric cancer. *Gastroenterology*. (2017) 152:2011–21. doi: 10.1053/j.gastro.2017.02.017
25. Chitadze G, Lettau M, Luecke S, Wang T, Janssen O, Furst D, et al. NKG2D- and T-cell receptor-dependent lysis of malignant glioma cell lines by human gammadelta T cells: modulation by tomosolamide and A disintegrin and metalloproteases 10 and 17 inhibitors. *Oncotarget*. (2016) 5:e1093276. doi: 10.1080/2162402X.2015.1093276
26. Simoes AE, Di Lorenzo B, Silva-Santos B. Molecular determinants of target cell recognition by human gammadelta T Cells. *Front Immunol*. (2018) 9:929. doi: 10.3389/fimmu.2018.00929
27. Edge SB, Compton CC. The american joint committee on cancer: the 7th edition of the AJCC cancer staging manual and the future of TNM. *Ann Surg Oncol*. (2010) 17:1471–4. doi: 10.1245/s10434-010-0985-4
28. Wagner GP, Kin K, Lynch VJ. Measurement of mRNA abundance using RNA-seq data: RPKM measure is inconsistent among samples. *Theory Biosci*. (2012) 131:281–5. doi: 10.1007/s12064-012-0162-3
29. Dangaj D, Bruand M, Grimm AJ, Ronet C, Barras D, Duttagupta PA, et al. Cooperation between constitutive and inducible chemokines enables t cell engraftment and immune attack in solid tumors. *Cancer Cell*. (2019) 35:885–900 e10. doi: 10.1016/j.ccell.2019.05.004
30. Miao YR, Zhang Q, Lei Q, Luo M, Xie GY, Wang H, et al. ImmuCellAI: a unique method for comprehensive t-cell subsets abundance prediction and its application in cancer immunotherapy. *Adv Sci*. (2020) 7:1902880. doi: 10.1002/adv.201902880
31. Newman AM, Steen CB, Liu CL, Gentles AJ, Chaudhuri AA, Scherer F, et al. Determining cell type abundance and expression from bulk tissues with digital cytometry. *Nat Biotechnol*. (2019) 37:773–82. doi: 10.1038/s41587-019-0114-2
32. Qian BZ, Li J, Zhang H, Kitamura T, Zhang J, Campion LR, et al. CCL2 recruits inflammatory monocytes to facilitate breast-tumour metastasis. *Nature*. (2011) 475:222–5. doi: 10.1038/nature10138
33. Zhou SL, Zhou ZJ, Hu ZQ, Huang XW, Wang Z, Chen EB, et al. Tumor-Associated neutrophils recruit macrophages and t-regulatory cells to promote progression of hepatocellular carcinoma and resistance to sorafenib. *Gastroenterology*. (2016) 150:1646–58.e17. doi: 10.1053/j.gastro.2016.02.040
34. Chung AS, Wu X, Zhuang G, Ngu H, Kasman I, Zhang J, et al. An interleukin-17-mediated paracrine network promotes tumor resistance to anti-angiogenic therapy. *Nat Med*. (2013) 19:1114–23. doi: 10.1038/nm.3291
35. Oja AE, Vieira Braga FA, Remmerswaal EB, Kragten NA, Hertoghs KM, Zuo J, et al. The transcription factor hobit identifies human cytotoxic CD4(+) T Cells. *Front Immunol*. (2017) 8:325. doi: 10.3389/fimmu.2017.00325
36. Ajuebor MN, Jin Y, Gremillion GL, Strieter RM, Chen Q, Adegbeyegba PA. GammadeltaT cells initiate acute inflammation and injury in adenovirus-infected liver via cytokine-chemokine cross talk. *J Virol*. (2008) 82:9564–76. doi: 10.1128/JVI.00927-08
37. Moser B, Eberl M. gammadelta T-APCs: a novel tool for immunotherapy? *Cell Mol Life Sci*. (2011) 68:2443–52. doi: 10.1007/s00018-011-0706-6
38. Gajewski TF, Schreiber H, Fu YX. Innate and adaptive immune cells in the tumor microenvironment. *Nat Immunol*. (2013) 14:1014–22. doi: 10.1038/ni.2703
39. Gentles AJ, Newman AM, Liu CL, Bratman SV, Feng W, Kim D, et al. The prognostic landscape of genes and infiltrating immune cells across human cancers. *Nat Med*. (2015) 21:938–45. doi: 10.1038/nm.3909
40. Meraviglia S, Eberl M, Vermijlen D, Todaro M, Buccheri S, Cicero G, et al. *In vivo* manipulation of Vgamma9Vdelta2 T cells with zoledronate and low-dose interleukin-2 for immunotherapy of advanced breast cancer patients. *Clin Exp Immunol*. (2010) 161:290–7. doi: 10.1111/j.1365-2249.2010.04167.x
41. Li H, Pauza CD. Rapamycin increases the yield and effector function of human gammadelta T cells stimulated *in vitro*. *Cancer Immunol Immunother*. (2011) 60:361–70. doi: 10.1007/s00262-010-0945-7
42. Xiang Z, Tu W. Dual face of V γ 9V δ 2-T cells in tumor immunology: anti- versus pro-tumoral activities. *Front Immunol*. (2017) 8:1041. doi: 10.3389/fimmu.2017.01041
43. Caccamo N, Todaro M, Sireci G, Meraviglia S, Stassi G, Dieli F. Mechanisms underlying lineage commitment and plasticity of human $\gamma\delta$ T cells. *Cell Mol Immunol*. (2013) 10:30–4. doi: 10.1038/cmi.2012.42
44. Wesch D, Peters C, Siegers GM. Human gamma delta T regulatory cells in cancer: fact or fiction? *Front Immunol*. (2014) 5:598. doi: 10.3389/fimmu.2014.00598
45. Cai XY, Wang JX, Yi Y, He HW, Ni XC, Zhou J, et al. Low counts of $\gamma\delta$ T cells in peritumoral liver tissue are related to more frequent recurrence in patients with hepatocellular carcinoma after curative resection. *APJCP*. (2014) 15:775–80. doi: 10.7314/APJCP.2014.15.2.775
46. Wang J, Lin C, Li H, Li R, Wu Y, Liu H, et al. Tumor-infiltrating $\gamma\delta$ T cells predict prognosis and adjuvant chemotherapeutic benefit in patients with gastric cancer. *Oncotarget*. (2017) 6:e1353858. doi: 10.1080/2162402X.2017.1353858
47. Ma C, Zhang Q, Ye J, Wang F, Zhang Y, Wevers E, et al. Tumor-infiltrating $\gamma\delta$ T lymphocytes predict clinical outcome in human breast cancer. *J Immunol*. (2012) 189:5029–36. doi: 10.4049/jimmunol.1201892
48. Paul S, Singh AK, Shilpi, Lal G. Phenotypic and functional plasticity of gamma-delta ($\gamma\delta$) T cells in inflammation and tolerance. *Int Rev Immunol*. (2014) 33:537–58. doi: 10.3109/08830185.2013.863306
49. Maniar A, Zhang X, Lin W, Gastman BR, Pauza CD, Strome SE, et al. Human gammadelta T lymphocytes induce robust NK cell-mediated antitumor cytotoxicity through CD137 engagement. *Blood*. (2010) 116:1726–33. doi: 10.1182/blood-2009-07-234211
50. Shang B, Liu Y, Jiang SJ, Liu Y. Prognostic value of tumor-infiltrating FoxP3+ regulatory T cells in cancers: a systematic review and meta-analysis. *Sci Rep*. (2015) 5:15179. doi: 10.1038/srep15179
51. Mandal R, Senbabaoglu Y, Desrichard A, Havel JJ, Dalin MG, Riaz N, et al. The head and neck cancer immune landscape and its immunotherapeutic implications. *JCI Insight*. (2016) 1:e89829. doi: 10.1172/jci.insight.89829

52. Wherry EJ. T cell exhaustion. *Nat Immunol.* (2011) 12:492–9. doi: 10.1038/ni.2035
53. Simoni Y, Becht E, Fehlings M, Loh CY, Koo SL, Teng KWW, et al. Bystander CD8(+) T cells are abundant and phenotypically distinct in human tumour infiltrates. *Nature.* (2018) 557:575–9. doi: 10.1038/s41586-018-0130-2
54. Gameiro SF, Ghasemi F, Barrett JW, Koropatnick J, Nichols AC, Mymryk JS, et al. Treatment-naïve HPV+ head and neck cancers display a T-cell-inflamed phenotype distinct from their HPV- counterparts that has implications for immunotherapy. *Oncoimmunology.* (2018) 7:e1498439. doi: 10.1080/2162402X.2018.1498439
55. Fujii SI, Shimizu K. Immune networks and therapeutic targeting of iNKT cells in cancer. *Trends Immunol.* (2019) 40:984–97. doi: 10.1016/j.it.2019.09.008
56. Zhang Y, Springfield R, Chen S, Li X, Feng X, Moshirian R, et al. alpha-GalCer and iNKT cell-based cancer immunotherapy: realizing the therapeutic potentials. *Front Immunol.* (2019) 10:1126. doi: 10.3389/fimmu.2019.01126
57. Arnett HA, Viney JL. Immune modulation by butyrophilins. *Nat Rev Immunol.* (2014) 14:559–69. doi: 10.1038/nri3715
58. Smith IA, Knezevic BR, Ammann JU, Rhodes DA, Aw D, Palmer DB, et al. BTN1A1, the mammary gland butyrophilin, and BTN2A2 are both inhibitors of T cell activation. *J Immunol.* (2010) 184:3514–25. doi: 10.4049/jimmunol.0900416
59. Ammann JU, Cooke A, Trowsdale J. Butyrophilin Btn2a2 inhibits TCR activation and phosphatidylinositol 3-kinase/Akt pathway signaling and induces Foxp3 expression in T lymphocytes. *J Immunol.* (2013) 190:5030–6. doi: 10.4049/jimmunol.1203325
60. Karunakaran MM, Willcox CR, Salim M, Paletta D, Fichtner AS, Noll A, et al. Butyrophilin-2A1 directly binds germline-encoded regions of the Vgamma9Vdelta2 TCR and is essential for phosphoantigen sensing. *Immunity.* (2020) 52:487–98.e6. doi: 10.1016/j.immuni.2020.02.014
61. Freed-Pastor WA, Mizuno H, Zhao X, Langerod A, Moon SH, Rodriguez-Barrueco R, et al. Mutant p53 disrupts mammary tissue architecture via the mevalonate pathway. *Cell.* (2012) 148:244–58. doi: 10.1016/j.cell.2011.12.017
62. Gober HJ, Kistowska M, Angman L, Jenö P, Mori L, De Libero G. Human T cell receptor gammadelta cells recognize endogenous mevalonate metabolites in tumor cells. *J Exp Med.* (2003) 197:163–8. doi: 10.1084/jem.20021500
63. Gruenbacher G, Nussbaumer O, Gander H, Steiner B, Leonhartsberger N, Thurnher M. Stress-related and homeostatic cytokines regulate Vgamma9Vdelta2 T-cell surveillance of mevalonate metabolism. *Oncoimmunology.* (2014) 3:e953410. doi: 10.4161/21624011.2014.953410
64. Harly C, Guillaume Y, Nedellec S, Peigne CM, Monkkonen H, Monkkonen J, et al. Key implication of CD277/butyrophilin-3 (BTN3A) in cellular stress sensing by a major human gammadelta T-cell subset. *Blood.* (2012) 120:2269–79. doi: 10.1182/blood-2012-05-430470
65. Sandstrom A, Peigne CM, Leger A, Crooks JE, Konczak F, Gesnel MC, et al. The intracellular B30.2 domain of butyrophilin 3A1 binds phosphoantigens to mediate activation of human Vgamma9Vdelta2 T cells. *Immunity.* (2014) 40:490–500. doi: 10.1016/j.immuni.2014.03.003
66. Yang Y, Li L, Yuan L, Zhou X, Duan J, Xiao H, et al. A structural change in butyrophilin upon phosphoantigen binding underlies phosphoantigen-mediated Vgamma9Vdelta2 T Cell Activation. *Immunity.* (2019) 50:1043–53.e5. doi: 10.1016/j.immuni.2019.02.016
67. Sebestyen Z, Scheper W, Vyborova A, Gu S, Rychnavska Z, Schiffler M, et al. RhoB mediates phosphoantigen recognition by Vgamma9Vdelta2 T Cell Receptor. *Cell Rep.* (2016) 15:1973–85. doi: 10.1016/j.celrep.2016.04.081
68. Rhodes DA, Chen HC, Price AJ, Keeble AH, Davey MS, James LC, et al. Activation of human gammadelta T cells by cytosolic interactions of BTN3A1 with soluble phosphoantigens and the cytoskeletal adaptor periplakin. *J Immunol.* (2015) 194:2390–8. doi: 10.4049/jimmunol.1401064
69. Le Page C, Marineau A, Bonza PK, Rahimi K, Cyr L, Labouba I, et al. BTN3A2 expression in epithelial ovarian cancer is associated with higher tumor infiltrating T cells and a better prognosis. *PLoS ONE.* (2012) 7:e38541. doi: 10.1371/journal.pone.0038541
70. Wrobel P, Shojaei H, Schitteck B, Gieseler F, Wollenberg B, Kalthoff H, et al. Lysis of a broad range of epithelial tumour cells by human gamma delta T cells: involvement of NKG2D ligands and T-cell receptor-versus NKG2D-dependent recognition. *Scand J Immunol.* (2007) 66:320–8. doi: 10.1111/j.1365-3083.2007.01963.x
71. Marten A, von Lilienfeld-Toal M, Buchler MW, Schmidt J. Soluble MIC is elevated in the serum of patients with pancreatic carcinoma diminishing gammadelta T cell cytotoxicity. *Int J Cancer.* (2006) 119:2359–65. doi: 10.1002/ijc.22186

Conflict of Interest: The authors declare that the research was conducted in the absence of any commercial or financial relationships that could be construed as a potential conflict of interest.

Copyright © 2020 Lu, Dai, Guo, Wang, Wen, Yang, Lin, Xie, Wen, Fang and Wang. This is an open-access article distributed under the terms of the Creative Commons Attribution License (CC BY). The use, distribution or reproduction in other forums is permitted, provided the original author(s) and the copyright owner(s) are credited and that the original publication in this journal is cited, in accordance with accepted academic practice. No use, distribution or reproduction is permitted which does not comply with these terms.